On the physical properties of BIOPOL/ethylene-vinyl acetate blends*

F. Gassner and A. J. Owen§
Institut Physik III, Universität Regensburg, 8400 Regensburg, Germany
(Received 1 May 1991; revised 18 November 1991; accepted 24 February 1992)

Some aspects of the structural, thermal and mechanical properties of ethylene-vinyl acetate (EVA) blended with biodegradable BIOPOL copolymers have been investigated in this work. X-ray measurements and thermal analysis showed that a homogeneous mixture of the two components was not formed: two crystalline structures, melting regions and glass transitions were found, relating to the BIOPOL and EVA components separately. Phase separation was also investigated by scanning electron microscopy of plasma-etched and biodegraded samples. Dynamic mechanical measurements showed that the EVA component reduced the dynamic modulus over the whole temperature range of measurement. The fracture behaviour was markedly dependent on blend composition. Weight loss measurements of soil-degraded samples indicated that only the BIOPOL component degraded biologically.

(Keywords: BIOPOL/EVA blends; PHB/HV copolymers; physical properties; biodegradable)

INTRODUCTION

An important objective of research in the field of polymer blends is to understand the physical effects which occur when different polymer species are mixed. By suitable choice of composition and processing conditions, polymer blends can often be tailor-made to have specific and desirable properties.

This paper is part of a study on the properties of blends based on bacterially produced poly(3-hydroxybutyrate-*co*-3-hydroxyvalerate) (PHB/HV) (tradename BIOPOL, ICI Biological Products). These PHB/HV copolymers are biodegradable and show a wide range of properties depending on the HV content[1]. However, they suffer from some disadvantages compared to conventional thermoplastics such as polyethylene (PE) and polypropylene: they are relatively expensive to produce, and the temperature conditions under which they can be processed are limited. By blending BIOPOL with other, cheaper thermoplastics, however, the possibility of obtaining inexpensive materials with improved processability can be explored.

Martuscelli and co-workers have shown that the bacterial homopolymer PHB is miscible in the melt with poly(ethylene oxide) (PEO)[2] and poly(vinyl acetate), but not with ethylene–propylene copolymer[3]. Dave *et al.*[4] showed using d.s.c. measurements that the bacterial copolymer PHB/16%HV is completely immiscible with polystyrene, poly(ε-caprolactone) and poly(L-lactide), partially miscible with styrene-acrylonitrile and acrylonitrile-butadiene-styrene, and completely miscible with poly(vinyl chloride) (PVC).

Another candidate for blending with BIOPOL is the ethylene-vinyl acetate (EVA) system. Vinyl acetate (VA) copolymerized with PE reduces the crystallinity of PE, resulting in a softer, more rubbery material. EVA itself is miscible with PVC over a range of VA contents[5], and is used commercially as a plasticizer for PVC.

In this work blends of EVA with PHB/HV were investigated, with the aim of determining the miscibility behaviour of the two components, and the effects on the structural and mechanical properties in relation to the biodegradability behaviour.

EXPERIMENTAL

Materials and methods

Injection-moulded bars (100 mm × 12.5 mm × 3 mm) of blends of bacterially produced PHB/HV (BIOPOL) and synthetic EVA were provided by ICI Biological Products Division, Billingham, UK. For the present work a single PHB/HV composition (15 mol% HV) was chosen containing 1% boron nitride as nucleating agent and glycerine triacetate as plasticizer. The EVA copolymer used contained 28 mol% VA. The blends of PHB/HV and EVA were obtained by melt blending using a single screw extruder.

For most of the measurements, the 3 mm thick injection-moulded bars were remelted at 195°C and compression-moulded into thinner (0.7 mm thick) sheets which were quenched into cold water. These sheets were subsequently stored at room temperature (20°C). Individual specimens were stamped out of these sheets for further measurements.

The crystalline structure was characterized by wide-angle X-ray scattering (WAXS) using monochromatic CuKα radiation and a position-sensitive detector.

Differential thermal analysis (d.t.a.) was carried out using Mettler equipment at a heating rate of 5°C min^{-1} from −60 to 200°C. This temperature range covered the glass transitions of both PHB/HV and EVA, as well as the melting transitions of both components.

*Paper presented at 'Polymer Physics', 3–5 April 1991, Bristol, UK
§To whom correspondence should be addressed

0032-3861/92/122508-05

Scanning electron microscopy (SEM) of degraded and undegraded samples was performed using a Philips model 500 scanning electron microscope. Samples were sputtered with a coating of gold and palladium using a Polaron cool sputter coater, in order to obtain a conducting specimen surface. Selected samples were plasma-etched prior to sputtering by exposure to activated oxygen in an r.f. field, using equipment developed at the Centre for Electron Microscopy, Graz, Austria[6].

The dynamic tensile modulus of various blend compositions was determined at a frequency of 5 Hz over a wide temperature range, using equipment designed and built in our laboratory. Stress–strain diagrams were obtained at a deformation rate of 1 mm min^{-1} with samples of length 55 mm, using a commercially available MINIMAT materials tester (Polymer Laboratories).

In addition, some simple soil-degradation tests were carried out. Samples were buried in soil consisting of 50 wt% potting compost, 25% horse manure and 25% leaf mould. The soil was watered and kept at 37°C and 90% relative humidity in an environmental chamber. At periodic intervals, samples were removed from the soil, lightly dusted-off and weighed. The weight loss due to microbial degradation was thereby measured as a function of time in the soil. Some samples were thoroughly cleaned in methanol, to remove all microbial growth, while others were investigated by SEM with their microbial growth on the surface for comparison (see later).

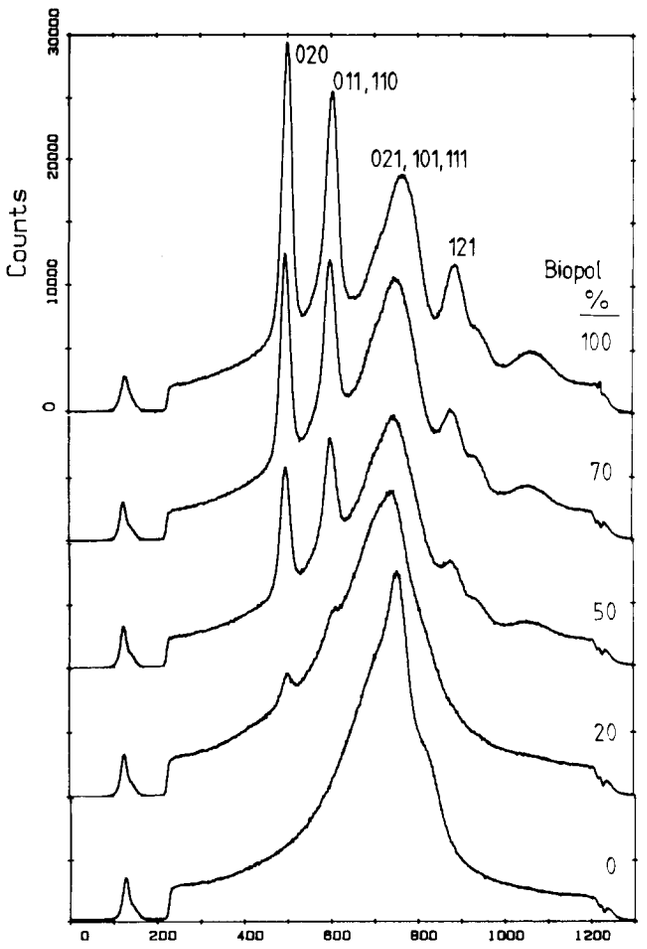

Figure 1 WAXS scattering patterns for BIPOL/EVA blends of various compositions

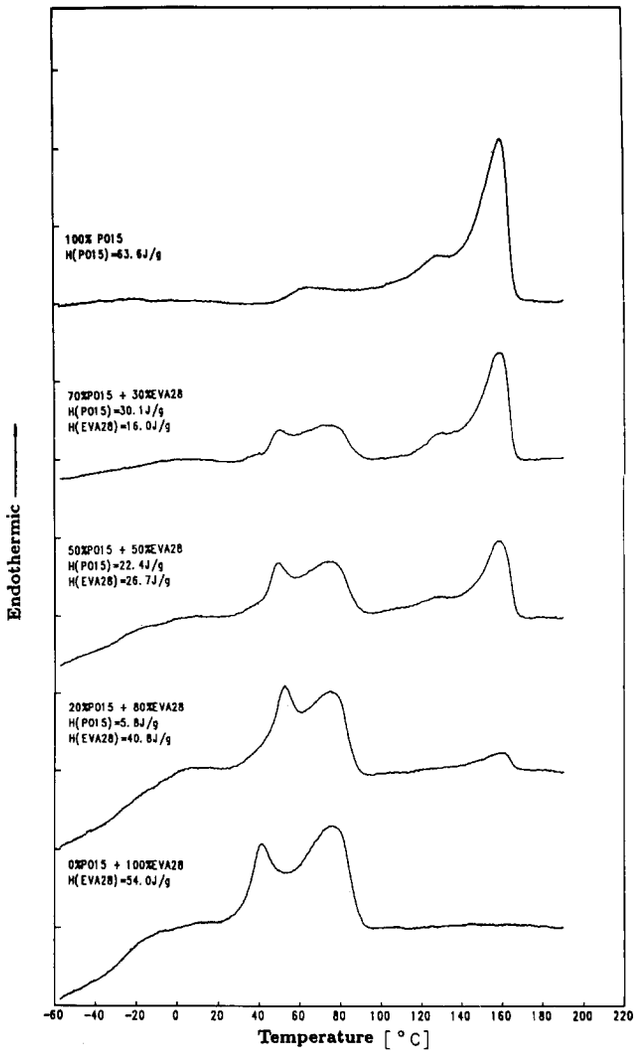

Figure 2 D.t.a. of BIOPOL/EVA blends of various compositions

RESULTS AND DISCUSSION

Wide-angle X-ray scattering

The PHB/HV samples showed the characteristic WAXS reflections of the PHB homopolymer crystal structure, a finding which is known from previous work[7–9] (*Figure 1*). It is believed that some of the HV monomer units co-crystallize in the PHB crystal lattice, producing some lattice distortion, while other HV units are excluded into the amorphous regions.

The X-ray scattering pattern for plain EVA (*Figure 1*) showed a broad amorphous halo together with an indication of two crystalline reflections with the same Bragg spacings as the (110) and (200) reflections of PE; it is clear that EVA is not fully amorphous, but shows some molecular ordering with poor crystalline perfection (see also d.t.a. results later).

The blends of PHB/HV and EVA showed a mixture of the scattering patterns of the two pure copolymer structures, with no other reflections being apparent (*Figure 1*). The above results suggest that the two blend components did not co-crystallize, but formed separate crystalline phases.

Differential thermal analysis

D.t.a. measurements of PHB/HV showed a wide melting range commencing at ~60°C with a main maximum at ~160°C (*Figure 2*). The blends exhibited

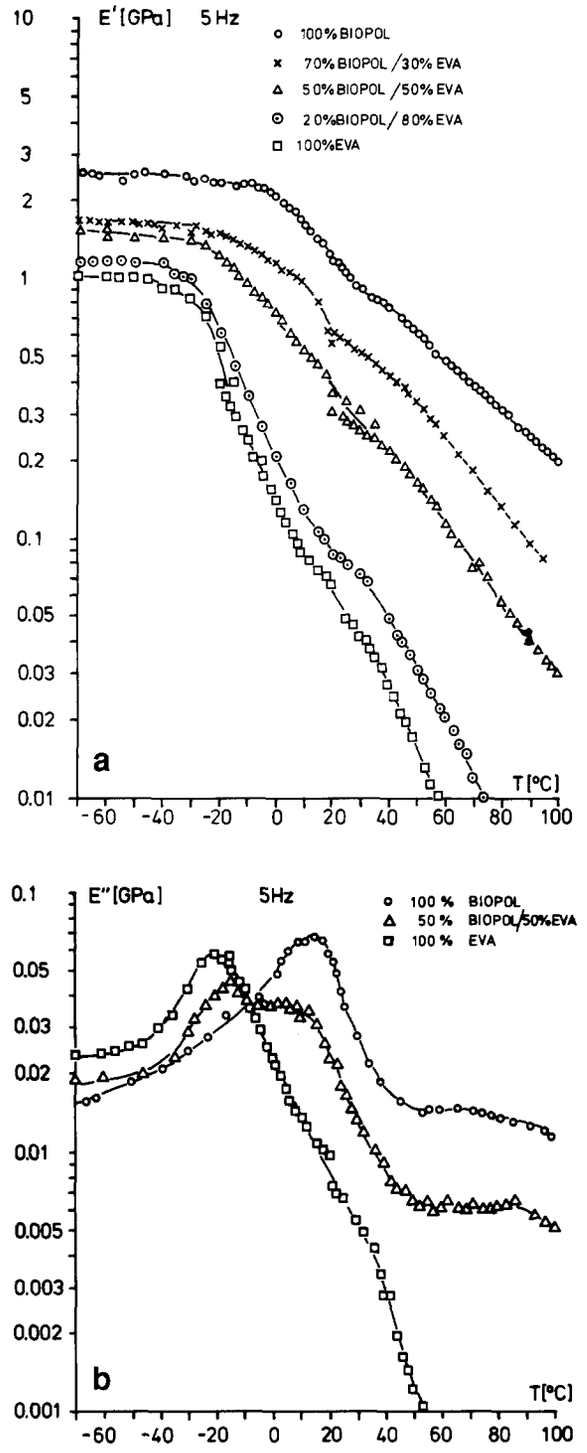

Figure 3 (a) Real and (b) imaginary parts of the dynamic modulus of various BIOPOL/EVA blends

an additional melting region consisting of two peaks between 40°C and 90°C, both relating to the EVA component. The crystallinity of the PHB/HV component was lowered considerably by blending with EVA: the melting enthalpy fell from 64 J g^{-1} in plain PHB/HV to 29 J g^{-1} of PHB/HV for the blend containing 20% PHB/HV. On the other hand, the EVA crystallinity was not affected significantly by the presence of PHB/HV: the melting enthalpy of the EVA was constant at ~53 J g^{-1} of EVA, irrespective of PHB/HV content. The degree of crystallinity of the EVA component was approximately constant at 20% (based on the melting enthalpy of PE, ~270 J g^{-1}).

The glass transition of plain PHB/HV was hardly noticeable in the d.t.a. diagram (*Figure 2*), presumably because the PHB/HV was highly crystalline. For the plain EVA sample a marked glass transition step was observed at ~ −25°C (*Figure 2*). Two weak steps in the d.t.a. curves were observed for the blends (*Figure 2*), presumably due to EVA at ~ −25°C and PHB/HV at 5°C. However, these transitions were not very clearly defined. Since a homogeneous amorphous region would show a single glass transition between the transitions for the pure components, it is concluded that the two blend components do not form a homogeneous amorphous phase.

The above results on miscibility are to be expected if the solubility parameters (δ) of the two components are considered. Using data from Van Krevelen[10], we estimate δ for PHB/15%HV to be 9.35 $cal^{1/2}$ $cm^{-3/2}$, while for EVA it is much lower (8.38 $cal^{1/2}$ $cm^{-3/2}$). The difference is presumably too great to allow significant miscibility in the BIOPOL/EVA system. PHB homopolymer on the other hand has a δ of 9.41, which is relatively close to the δ for PEO of 9.54; miscibility was indeed observed for that system[2].

Dynamic mechanical measurements

Results are shown in *Figure 3* for five BIOPOL/EVA blend compositions. The real part of the dynamic tensile modulus E' is highest in the plain PHB/HV material over the whole temperature range. At ~5°C it starts to fall rapidly due to the onset of amorphous softening at the glass transition. This is seen as a maximum in the imaginary part E'' (β-relaxation), which occurs at ~15°C. For the plain EVA there is a relaxation maximum at ~ −20°C, which is due to the glass transition of EVA. The plain EVA is softer than PHB/HV throughout; EVA melts at > ~50°C, so the modulus falls rapidly in this temperature region.

Only three E'' curves have been shown in *Figure 3* for the sake of clarity. Two relaxation transitions occurred in the blends, rather than a single transition, in agreement with the d.t.a. measurements. However, the E'' peaks were slightly shifted towards each other.

Stress–strain measurements

Figure 4 summarizes the results of stress–strain measurements. In the composition region marked A

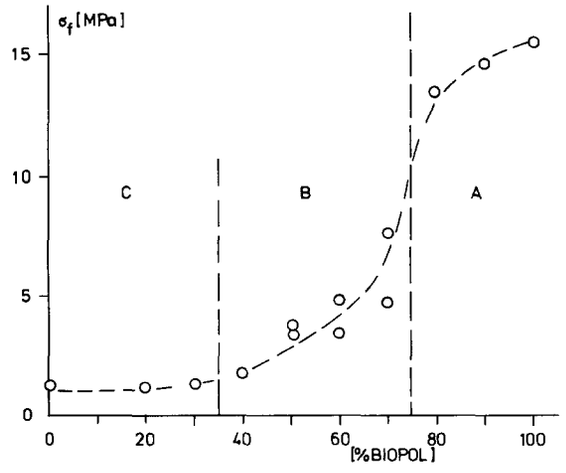

Figure 4 Maximum stress *versus* BIOPOL content (elongation rate 1 mm min^{-1})

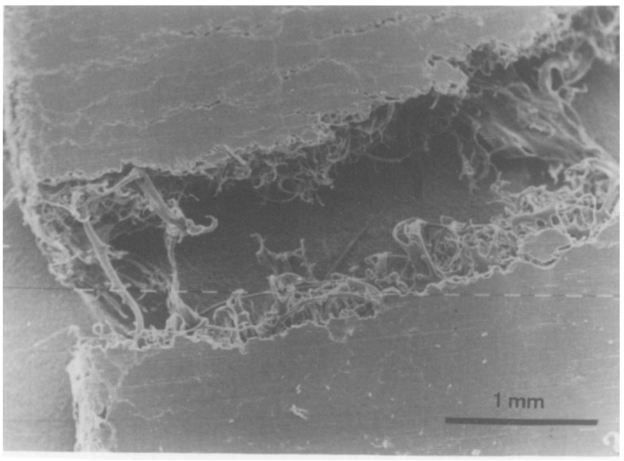

Figure 5 SEM micrograph of failure surface of a 70:30 BIOPOL/EVA blend showing some EVA fibrils spanning the crack

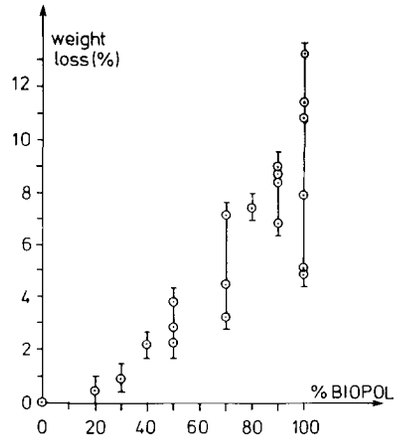

Figure 6 Weight loss due to microbial attack for 4 weeks as a function of BIOPOL content

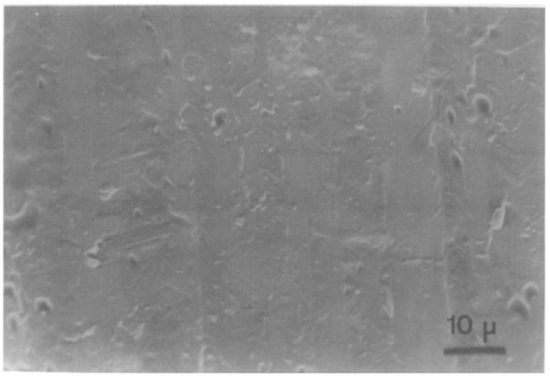

Figure 7 SEM micrograph of an untreated 90:10 BIOPOL/EVA blend

(high PHB/HV content) the samples showed brittle fracture at ~1% strain; the failure stress is shown plotted against BIOPOL content. In region C (high EVA content) there was considerable plastic deformation at low stress levels. Samples could be extended to high draw ratios (several 100% strain without fracturing). The stress given is that where the stress–strain diagram significantly deviates from the initial linear behaviour. In the intermediate region B, it was clear that the EVA matrix deformed plastically, while the PHB/HV remained virtually undeformed. The stress–strain diagrams showed a marked stress maximum. Scanning electron micrographs of these samples showed fibrillar regions of stretched EVA spanning the failure region (*Figure 5*).

Degradation tests

Soil-degradation test results are summarized in *Figure 6*. The weight loss due to microbial degradation after exposure for 4 weeks has been plotted as a function of BIOPOL content. Each circle refers to a single sample, the weight being measurable to an accuracy of ~0.5%. The scatter in the results at any particular PHB/HV content appeared to be related to the position of the sample in the soil: those in the wettest positions showed the most weight loss. Since it became difficult to control the moisture content accurately, these measurements were discontinued after 4 weeks. Nevertheless, there is a clear correlation between weight loss and BIOPOL content, showing convincingly that the BIOPOL component alone is being degraded in the soil, leaving EVA undegraded. Thus, these materials must be regarded as being biodestructible (or biodisintegrating) rather than biodegradable. Further work is being directed at ascertaining whether or not the degradation behaviour can be affected significantly by thermal or other treatment.

Figures 7–12 show a series of representative scanning electron micrographs of untreated and degraded samples. The surface of the untreated sample (*Figure 7*) was relatively smooth. *Figure 8* shows some microbial growth on a 40:60 BIOPOL/EVA sample. The small round

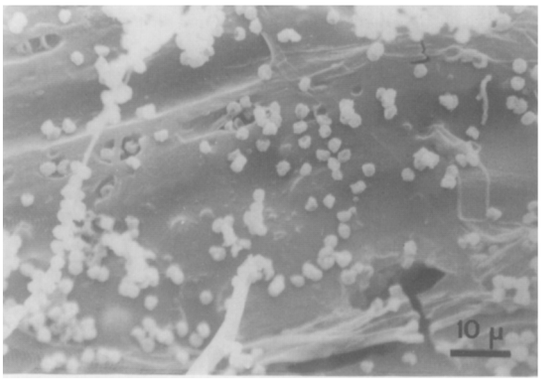

Figure 8 SEM micrograph of a 40:60 BIOPOL/EVA blend after microbial attack for 4 weeks

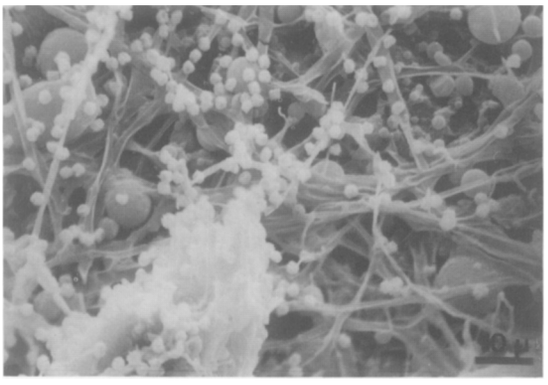

Figure 9 SEM micrograph of a 90:10 BIOPOL/EVA blend after microbial attack for 4 weeks

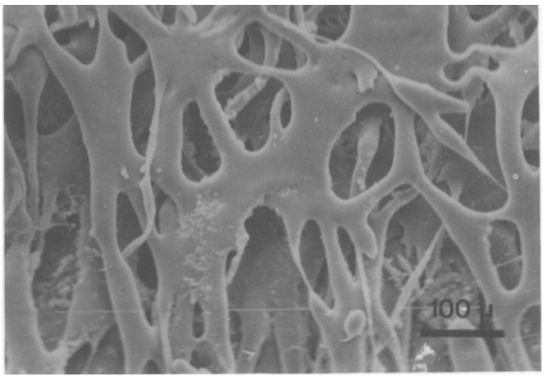

Figure 10 SEM micrograph of a 60:40 BIOPOL/EVA blend after microbial attack for 4 weeks

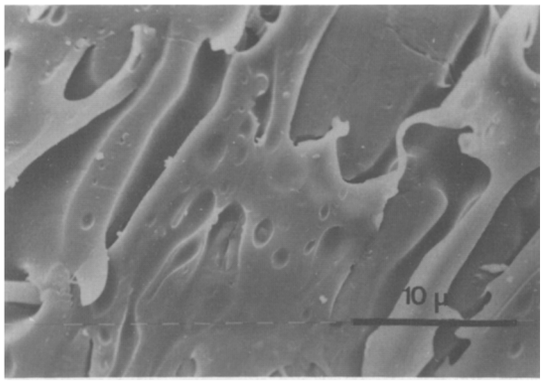

Figure 11 SEM micrograph of a plasma-etched 60:40 BIOPOL/EVA blend

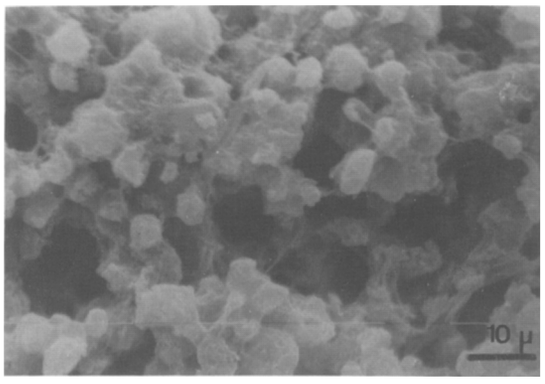

Figure 12 SEM micrograph of plain BIOPOL after microbial attack for 4 weeks

objects ~0.2 μm in diameter are thought to be bacteria, whereas the strands are fungal growth or fine roots[11] (see *Figure 9*). *Figure 10* is a 60:40 blend which has been cleaned. Here a cellular or sponge-like morphology is seen; the BIOPOL component had been eaten away, leaving a fairly smooth EVA component. This observation could be substantiated by optical microscopy measurements using a polarizing microscope, where it was possible to distinguish between BIOPOL and EVA components in thin films by their different birefringent behaviour. Those results, not shown here, will be the subject of a future paper. *Figure 11* shows the same sample after plasma etching, again indicating phase separation and selective etching. A plain BIOPOL sample after microbial attack is shown in *Figure 12*. In this case one sees the indication of a spherulitic texture in the interior of the sample. It is clear that the selective biological etching of the BIOPOL component provides an interesting means of investigating the internal morphology of such blends at this level of magnification.

CONCLUSIONS

The partially crystalline solid blends of BIOPOL and EVA showed two glass transitions and melting regions, relating to the two separate components. The dynamic modulus and failure strength were strongly affected by blend composition. In the region above ~70% BIOPOL, samples were stiff and relatively brittle, the behaviour being dominated by the BIOPOL component. Below ~70% BIOPOL, the behaviour was dominated by the softer EVA component, which appears to form a continuous matrix in which BIOPOL domains are embedded. Only the BIOPOL component showed degradation in soil-degradation tests. Further work is now in progress to obtain more comprehensive data on mechanical properties and to relate these to the structure.

ACKNOWLEDGEMENTS

Thanks are due to the Deutsche Forschungsgemeinschaft for financially supporting this work. The authors also thank Professor R. Bonart for encouraging the work, H. Zott for obtaining X-ray measurements and A. Webb of ICI for providing samples. Professor Winter, Professor Molitoris and Dr Matavulj of the Biology Department, Regensburg University are thanked for their co-operation in identifying microbial growth.

REFERENCES

1 Holmes, P. A. in 'Developments in Crystalline Polymers-2' (Ed. D. C. Bassett), Elsevier, 1988, Ch. 1
2 Avella, M. and Martuscelli, E. *Polymer* 1988, **29**, 1731
3 Greco, P. and Martuscelli, E. *Polymer* 1989, **30**, 1475
4 Dave, P. B., Gross, R. A. and McCarthy, S. P. 'ANTEC '90', Society of Plastics Engineers, 1990, pp. 1439–1442
5 Paul, D. R. and Barlow, J. W. *Polymer* 1984, **25**, 487
6 Aldrian, A., Jakopic, E., Reiter, O. and Ziegelbecker, R. 'Radex-Rundschau', Österreichisch. Amerikanische Magnesit A. G., Radenthein, Austria, Vol. 2, 1967
7 Bloembergen, S., Holden, D. A., Hamer, G. K., Bluhm, T. L. and Marchessault, R. H. *Macromolecules* 1986, **19**, 2865
8 Bauer, H. and Owen, A. J. *Colloid Polym. Sci.* 1988, **266**, 241
9 Barker, P. A., Mason, F. and Barham, P. J. *J. Mater. Sci.* 1990, **25**, 1952
10 Van Krevelen, D. W. 'Properties of Polymers', Elsevier, Amsterdam, 1972
11 Winter, J., Molitoris, P. and Matavulj, M. personal communication, 1991